APPLIED GEOPHYSICS, Vol.13, No.2 (June 2016), P. 227-237, 5 Figures.
DOI:10.1007/s11770-016-0552-2

Aeromagnetic data and geological structure of continental China: A review*

Xiong Sheng-Qing♦[1,2,3], Tong Jing[2], Ding Yan-Yun[1], and Li Zhan-Kui[1]

Abstract: We review the latest aeromagnetic geological data of continental China. We discuss the latest achievements in geological mapping and the newly detected features based on aeromagnetic data. Using aeromagnetic data collected for more than 50 years, a series of 1:5000000 and 1:1000000 aeromagnetic maps of continental China were compiled using state-of-the-art digital technology, and data processing and transformation. Guided by plate tectonics and continental dynamics, rock physical properties, and magnetic anomalies, we compiled maps of the depth of the magnetic basement of continental China and the major geotectonic units, and presented newly detected geological structures based on the aeromagnetic data.
Keywords: regional aeromagnetic anomalies, magnetic basement, faults, magmatic rocks, structural units

Introduction

Regional aeromagnetic data are used to study geological structures. The aeromagnetic anomalies map of China and its adjacent seas on the scale of 1:4000000 (Liu et al., 1989) and the aeromagnetic ΔT anomaly map of China and its adjacent seas on the scale of 1:5000000 (Wang et al., 2004) have been compiled and published. Because of the acquisition of new high-precision aeromagnetic data and improvements in data processing, compiling, and interpretation over the last decade, it is necessary to compile a new national aeromagnetic anomalies map to satisfy the current requirements for precision and quality. Thus, we compiled aeromagnetic maps on the scale of 1:5000000 and 1:1000000 by applying advanced compilation technology and potential field data processing. The 1:5000000 aeromagnetic maps of continental China (Xiong et al., 2013a) are now published, and a new version of the 1:2500000 aeromagnetic maps of continental China will also be published.

Regional aeromagnetic data are used to study geological structures, outline regional tectonic units,

Manuscript received by the Editor November 10, 2015; revised manuscript received February 24, 2016.
*This work was supported by the China Land Aeromagnetic Characteristics and Tectonic Structures Research (No. 1212011087009), part of the national geological and mineral resources investigation projects, and the Comprehensive Exploration of Aero Geophysical & Remote Sensing Survey and Interpretation System Research (No. 2013AA063905), part of the planning for national high technology research and development.
1. China Aero Geophysical Survey & Remote Sensing Center for Land & Resources, Beijing 100083, China.
2. China University of Geosciences (Beijing), Beijing 100083, China.
3. Key Laboratory of Airborne Geophysics and Remote Sensing Geology, Ministry of Land and Resources, Beijing 100083, China.
♦Corresponding author: Xiong Sheng-Qing (Email: xsq@agrs.cn)

and detect mineral resources. Zhu (2013, unpublished) has compiled a national aeromagnetic map. Yang and Liang (2011, unpublished) also conducted a preliminary interpretation of the 2004 version of the national aeromagnetic ΔT anomalies map. Sun et al. (2001) studied key metallogenic belts using gravity and aeromagnetic data. Many others have studied regional geological structures using aeromagnetic data. However, no one has systematically discussed the geological features of continental China using aeromagnetic data and compiled the results into a map.

The maps compiled in this study describe the geological structures of continental China. Based on the 1:1000000 aeromagnetic maps, we study the regional geological features within the framework of plate tectonics and continental dynamics theory (Huang et al., 1985; Ren et al., 1999; Ren, 2003; Pan et al., 2009; Li, 2006, 2008; Wan, 2011; Ge et al., 2013; Liu, 2007; Teng et al., 2012; Zhao, 2009). We analyzed the aeromagnetic data and produced geological and structural maps. Based on these maps, we discuss the regional geology, the distribution of buried magmatic rocks, the magnetic properties of the basement, the thickness of the sedimentary cover, and the geotectonic framework.

We first discuss the compiled aeromagnetic maps of continental China, the magnetic map of the basement, the map of faults and magmatic rocks, and finally the map of regional tectonics. Because of length constraints, we only review the results without covering the theory and method of the data interpretation. All that will be discussed in detail in the forthcoming monograph "Aeromagnetic and geological structural characteristics of continental China based on 1:1000000 aeromagnetic maps."

Compilation of aeromagnetic maps of continental China

Based on the systematic analysis of 50 years of aeromagnetic data and using the latest high-precision aeromagnetic data, series of aeromagnetic maps were compiled using advanced digital, and data processing and transformation methods.

Data for mapping

The aeromagnetic data used are from 409 areas that cover 979.6 km^2 and were surveyed before 2011, including 143 high-precision and 266 medium–high-precision surveys (Figure 1). The high-precision magnetic data were acquired from the 1980s and up to 2011, using helium optically pumped magnetometers with ±1−3 nT precision, a GPS navigation system with precision of ±10 m, and a digital data acquisition system. The high-precision data concern 57.7% of the mapped areas (565.4 km^2). The medium-precision magnetic data were acquired from the 1970s to early 1980s, mainly

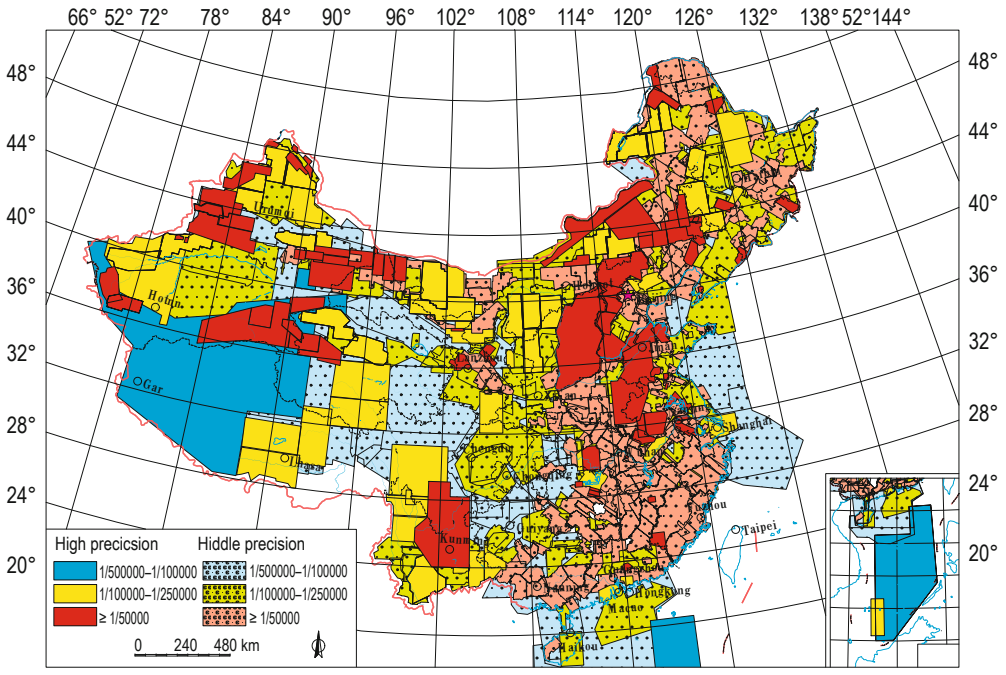

Fig.1 Aeromagnetic map of continental China and neighboring seas.

using proton magnetometers with precision of ±5−10 nT, positional accuracy of about ±100 m; the data concern 42.3% of the mapped areas (414.2 km^2).

Method of compilation

To compile the maps, we used the latest geophysical data processing and mapping software, including the GeoProbe Mager of the China Aero Geophysical Survey & Remote Sensing Center for Land & Resources, the Geosoft Oasis montaj software, and the MapGIS software.

The main map compilation techniques were the following (Xiong et al., 2013b). (1) Aeromagnetic data preprocessing and gridding for single-survey areas; magnetic diurnal variation correction and leveling was first applied prior to the 1 km × 1 km gridding. (2) Calculation of the base mapping altitude. The base altitude was finally set at 1000 m based on the potential field data processing. The lower altitude data in single-survey areas were transformed by upward continuation, whereas the higher altitude data were not transformed downward and the magnetic field was leveled based on the surrounding high-precision data. We did not perform high-pass filtering at 400 km and the new magnetic map maintains the regional magnetic features. (3) We constructed the grid framework and performed grid stitching by integrating, blending, and suturing (Wang, 2007). First, we used the high-precision data to construct the grid framework. Then, the framework was gradually stitched outward using different single-survey areas. Finally, the aeromagnetic ΔT grid data for China were compiled. This technique avoids the "seesaw" phenomenon in mapping owning to error accumulation and increases the reliability of the aeromagnetic data mapping. (4) Potential field transformation of the aeromagnetic ΔT grid data. In this study, we first the transformed the national aeromagnetic data, including the reduction to the magnetic pole of the conventional potential field data, and obtained the vertical derivative and up continuation. To delineate linear structures and the boundaries of magnetic bodies, we used the methods of tilt derivative, total horizontal derivative, total gradient mode, normalized total horizontal derivative, and vertical derivative. The reduction of the magnetic pole with variable inclination was applied to all data to increase the reliability of the transformation. Publicly available aeromagnetic data from neighboring countries were added to the aeromagnetic ΔT grid data of China before the transformation to reduce the number of false values in the desired rectangular area. For areas without any data, a new cosine limited method was applied to extend the data edge and reduce the effect of edge distortion, which improved the quality of the data transformation.

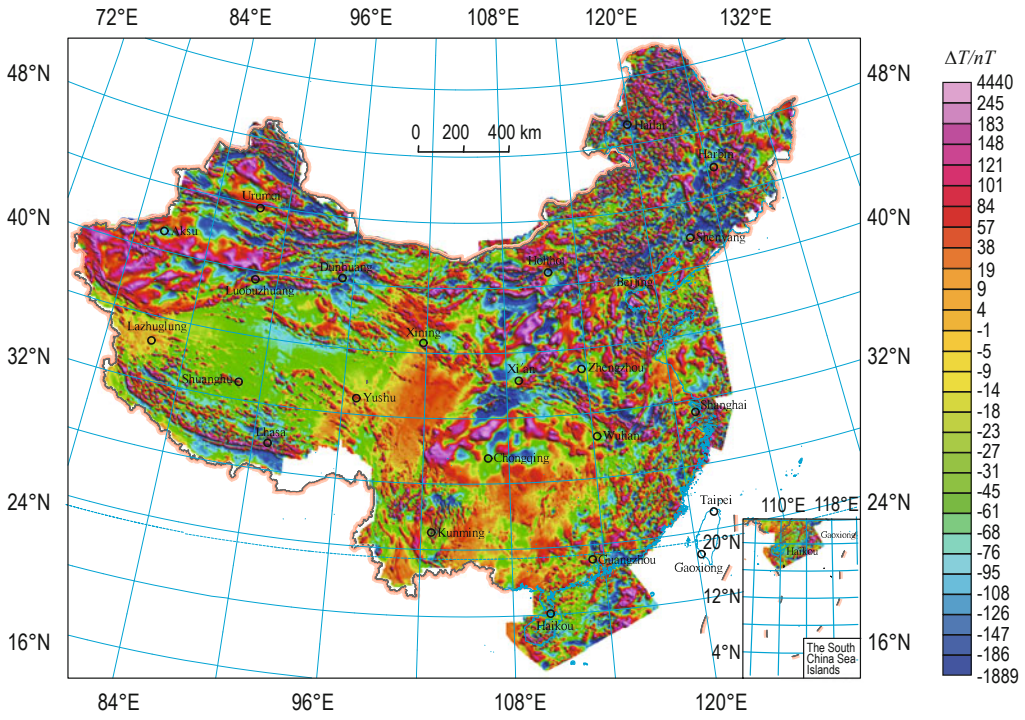

Fig.2 Stereo shaded-relief image of aeromagnetic ΔT data of continental China with magnetic pole reduction.

Compared with the aeromagnetic anomalies on the original ΔT aeromagnetic map, the positive magnetic anomalies increased on the stereo shaded-relief image of the continental aeromagnetic ΔT data of China with the reduction to the pole (Figure 2) owing to the elimination of the oblique magnetization. Many positive and negative magnetic anomalies were merged into one positive magnetic anomaly after processing, and the center of the positive anomaly was offset several degrees to the north, solving the problem of mismatch between the magnetic anomaly center and magnetic body in middle and low latitudes, which better shows the corresponding relation of the magnetic anomalies and geological structures in continental China, and helps detect faults and buried rocks and structures.

Compilation results

Compared with the 2004 1:5000000 aeromagnetic map of China, the main characteristics of the latest version are the following. (1) Serialization of the aeromagnetic maps. Seven types of maps, including the aeromagnetic ΔT map, the reduction-to-the-pole contour map, the vertical derivative with the reduction-to-the-pole contour map, the upward continuation of the 5 km, 10 km, 20 km, and 50 km contour maps, cover all the maps needed in geological studies. (2) Large quantities of high-precision aeromagnetic data. The new aeromagnetic data cover about 33.8 million km^2 and 75 survey areas with 40.5 million line km. (3) Higher resolution aeromagnetic data. Compared with the 2004 version with the 5 km × 5 km grid, the new grid space is 1 km × 1 km. This maintains the details of the regional magnetic data and does not require the use of high-pass filtering.

In brief, the compilation of old and new airborne magnetic maps and the use of the most advanced technology represent the current state-of-the-art national aeromagnetic surveys and processing methods.

Depth of magnetic basement of China based on aeromagnetic data

Methodology

About 120000 depth-related data of magnetic bodies were calculated from the original profiles of single-survey areas by using the tangent method (Zhu, 2002; Huang and Guo, 2007), the Vacquier method (Guan and An, 1991), Euler deconvolution (Guo et al., 2003), and other methods (Fan et al., 2010). Based on geological, including boreholes and petrophysics, and geophysical and seismic data, the depth of the Precambrian basement was found after eliminating the distortion of shallow magnetic bodies and volcanic rocks. Finally, we compiled the basement depth map of continental China based on the aeromagnetic data (Xiong et al., 2014a). By comparing the calculated basement depth (Figure 3) with the actual depth of Precambrian metamorphic and magmatic rocks in 162 boreholes, we find that the deviation is less than 20% in 91% of the cases, which satisfies the precision requirements.

Results and analysis

The magnetic basement depth map of continental China (Figure 3) mainly varies because of the large-scale magma intrusions and Precambrian metamorphics, and the variations in the distribution of sedimentary basins. The thickness and occurrence of Mesozoic and Paleozoic sedimentary rocks is also represented in the depth variations of the magnetic basement because the sedimentary cover is always above the magnetic basement. Thus, the map is of practical importance to oil and gas exploration in the basins (Xiong et al., 2014a).

The sedimentary cover is thin in eastern China and thick in western China. In the west, the thickness primarily ranges between 5000 m and 15000 m; nevertheless, the highest thickness is between 17000 m and 21000 m. Sedimentary rocks are found in the Junggar basin (5000−15000 m), Tuha Basin (5000−9000 m), Tarim Basin (7000−21000 m), Qaidamu Basin (5000−15000 m), the Hoh Xili-Song Pan depression (5000−13000 m), and in the basins and depressions of Tibet (5000−15000 m). In the east, the thickness of sedimentary cover ranges from 3000 m to 9000 m and, locally, reaches 11000 m. In eastern China, sedimentary rocks are found in the Erdos and Sicuan Basins (5000 −11000 m), the Jianghan Basin (3000−11000 m), the southern and northern depression of the Jiangnan uplift (3000−11000 m), the Simao and Chuxiong Basins (3000 −9000 m), the lower Yangtze and South Yellow Sea (3000 −9000 m), the Qinshui and the southern North China Basins (5000−9000 m), the Bohai Bay Basin (3000−9000 m), the Songliao Basin, the Hailaer and Erlian Basins (3000−9000 m), the Sanjiang River Basin (3000 −7000 m), the Zhujiangkou Basin, the southeastern Hainan Basin, the Yingge Sea Basin, and the North Gulf Basin (3000−9000 m). These basins and depressions have stable and thick sedimentary covers, and thus have high oil and gas potential.

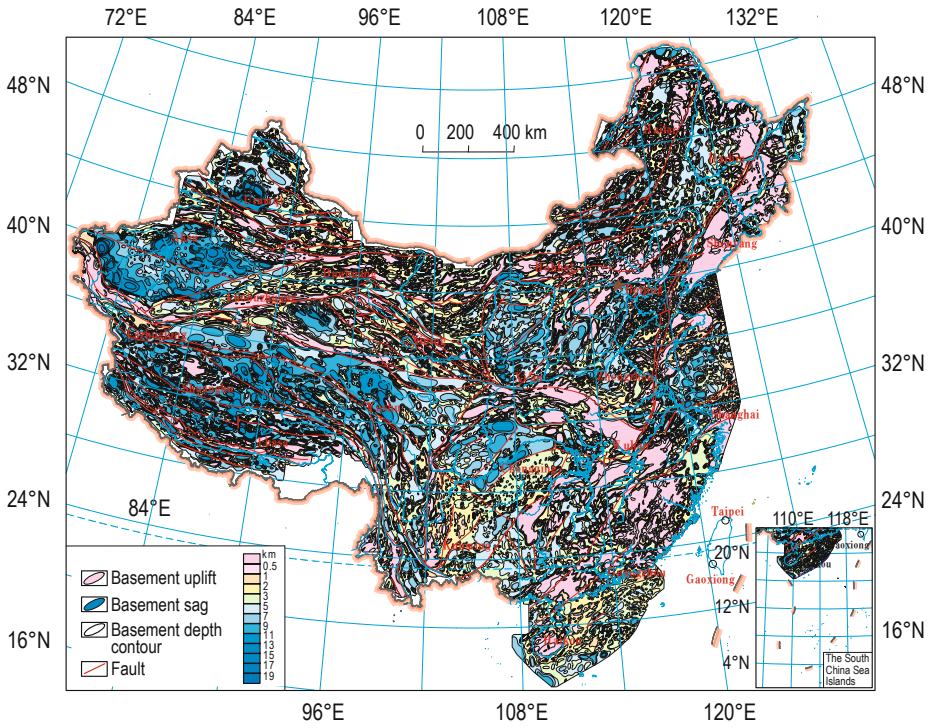

Fig.3 Basement depth map of continental China.

Distribution of faults and magmatic rocks in continental China based on aeromagnetic data

Methodology

1. How to recognize faults

Tectonic activity typically results in the vertical and horizontal displacement of the sedimentary cover and basement. Magmatic activity nearly always takes place along these displacements, alters the original geophysical field and Earth's surface, and is clearly seen in gravity and magnetic maps and remote-sensing images. Therefore, based on aeromagnetic, gravity, and remote-sensing data, faults can be detected.

We analyzed and compared aeromagnetic ΔT contour maps and related data to understand how faults are reflected on the magnetic map, and established the faults based on the multiple-scale variations of the magnetic anomalies. In addition, we compared detected and known faults on the gravity map and remote-sensing images to verify the accuracy.

2. Delineating magmatic rocks

To delineate magmatic rocks by using aeromagnetic data, one mainly relies on the magnetic differences of the magmatic rocks. The magnetic signal generally increases from felsic to mafic rocks; thus, compositional variations are reflected on the magnetic data, which allows to differentiate magmatic rocks of different compositions. The boundaries of magmatic bodies can be confirmed by the zero line of the aeromagnetic ΔT vertical first-order derivative with reduction to the pole and the gradient zone of tilt derivative with reduction to the pole.

The procedure for delineating buried magmatic rocks is as follows: first, we collect the magnetic data; second, we analyze and summarize the magnetic anomalies associated with known magmatic rocks; finally, we establish the interpretation procedure based on the correlation between magmatic anomalies and rock composition.

Results and analysis

1. Tectonic framework of continental China

In addition to the 1:1000000 aeromagnetic data and maps, we combined gravity and remote-sensing data. Consequently, we detected and confirmed 499 faults that we divided into deep faults (44), regional faults (46), and basement faults (409) (Figure 4).

The faults were divided into four systems and 25 series depending on their strike, activity, and scale by Cheng et al. (1994) and Ren et al. (1999):

(1) The Paleo-Asia fault system with nine series of faults: Khingan, Beishan–ErLian, Jungger, Tarim, Arkin, West Kunlun, Qilian–East Kunlun, and Qinling–Dabie Mountain.

(2) The Helan–Kang Dian fault system with three series of fault: Helan Mountain, Longmen Mountain, and Xikang Yunnan.

(3) The Tethyan fault system with four series of faults: Hoh Xili-Songpan, Qiangtang, Gangdise–Himalayan, and Sanjiang River.

(4) The Cathaysian–Pacific Rim fault system with nine series of faults: Huaying Mountain, Wuling–Xuefeng, Southeast Coast, Changbai Mountain–Shandong Peninsula, Northern Jiangsu, Southern Jiangsu, North China, Songliao, and the NW-trending Eastern China series of faults.

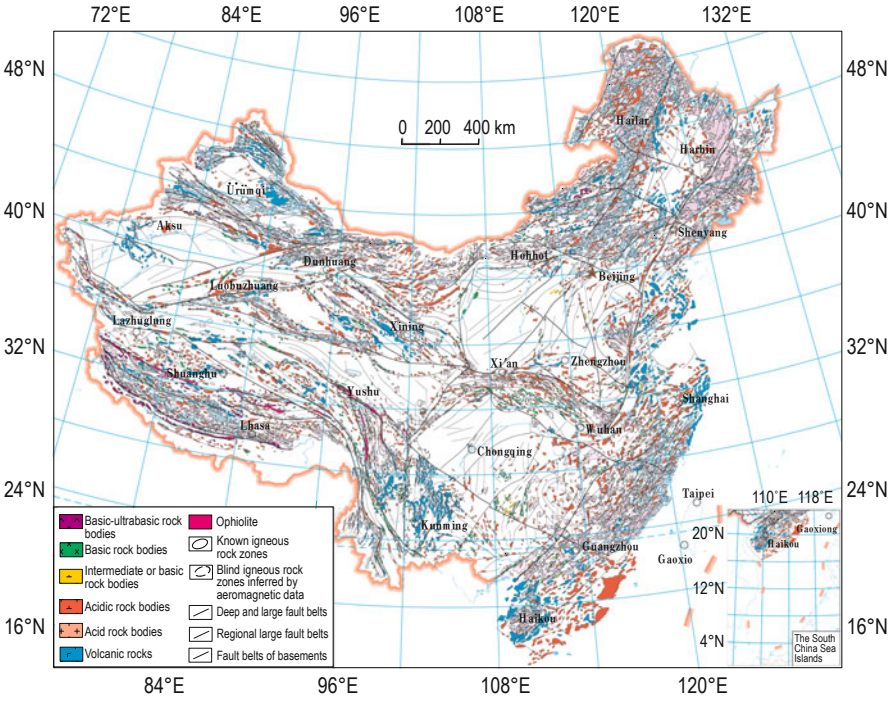

Fig.4 Distribution of faults and magmatic rocks in continental China based on aeromagnetic data.

2. New faults

In addition to the delineation of known faults, new faults were inferred by using the compiled magnetic maps, including the following large faults: Manzhouli–Yanji, Shangdu–Tangshan, Lanxian–Bengbu, Ankang–Nanchang, Weixin–Rongjiang, Baotou–Chaoyang Fault, Tongchuan–Fenyang, Hengshui–Fuyang, Shaoxing–Jiangshan–Beihai, HeliMuntain–Alxa Right Banner, Cele–Weiya, and Wudu–Kangding.

We also extended the Arkin Fault, the Jinsha River–Red River fault zone, the Nujiang River fault zone and the Kang Dian N–S structure.

(1) The Arkin fault belt

Cheng et al. (1994) believed that the Arkin Fault passes through the Beishan Mountain and then to Mongolia in the northeast and through the west Kunlun Mountain and India to the southwest. However, from the aeromagnetic map, the NEE-striking aeromagnetic anomaly zone of the Arkin Fault is terminated by NW-striking aeromagnetic anomalies in the Qiaowan area of eastern Anxi in the Gansu Province. In the southwest, it extends to Joan Muzitag at the eastern end of the western Kunlun Mountains.

(2) Western extension of the southwestern Sanjiang River fault belt

The published data suggest that the Tibet–Sanjiang River Fault strikes EW–NW and has a characteristic arc shape towards the northeast (Ren et al., 1999; Cheng et al., 1994; Li et al., 2008; Pan et al., 2002) in the Leiwuqi and Yushu areas. However, based on the magnetic and gravity data, and the regional geology, the Sanjiang River fault belt (Jinsha River Fault, Lancang River Fault, and Nujiang River Fault) does not turn to the west after extending to eastern Tibet but continues to the northwest and finally reaches the Buruoco and Xuelian Lake areas. This is a group of NW-trending faults that exists in the Tethyan fault system only. These faults were reoutlined and renamed as the Jinsha–Red

River fault belt, the Xuelian Lake–Lancang fault belt, and the Dingqing–Nujiang River fault belt. They have no relation with the EW-striking faults in Tibet and consist of two fault systems. These two groups of faults intersect each other in the Suo County and Zuogong. Therefore, the Pangong Tso–Nujiang River is renamed the Pangong Tso–Nyima deep fault in middle Tibet and intersects with the Dingqing–Nujiang River fault belt in Suoxian. The western segment of the Lazhulong–Jinsha River Fault is renamed the deep Lazhulong–Yushu Fault. The magnetic anomalies at the Jinsha River extend to the northwest and terminate in Yushu instead of turning to the west. This belt apparently cuts the magnetic anomalies belt of Lazhulong–Yushu with a displacement offset of up to 50 km based on the magnetic maps. The deep Xuelian Lake–Lancang River Fault extends to Geladandong and Xuelian Lake striking northwest; it does not pass through the Qiangtang Basin and it reaches the Shuanghu Lake and LongmuCo area. The NW-trending Dingqing–Nujiang River Fault passes Suoxian and reaches the Anduo area and, instead of turning to the west, continues to the northwest through the Qiangtang Basin before terminating at the Buruo Co area. The geological structures in Tibet are mainly controlled by the EW-trending faults, whereas the structures in the southwestern Sanjiang River area are mainly controlled by NW-trending faults. The two groups of deep faults form the tectonic framework of Tibet and southwest Sanjiang River (Xiong et al., 2014b). Geological evidence suggests that the arc-shaped structures in Tibet may be remnant of the Jurassic tectonic activity (Xiong et al., 2012).

(3) The northern and western extension of the NS-striking Xikang Yunnan fault belt

The Xikang Yunnan fault belt in the middle of China is believed to extend from the south to the north and reach Luding and Baoxing, and terminate at the NE-striking Longmen Mountain Fault. The fault belt does not continue to extend to the north and, in the east, ends at the Xiaojiang Fault and, in the west, ends at the Luzhijiang River Fault (Ren et al., 1999; Cheng et al., 1994). However, the new compiled aeromagnetic maps of the NS-striking Xikang Yunnan belt suggest a greater extend. The northern segment reaches the area of Songpan and the eastern segment reaches the Hunan Province in the south. Being the components of NS-striking fault system across central China, The Xikang Yunnan Fault exists since the Proterozoic and is part of the NS-striking faults that divide central China, and affects the formation and migration of oil and gas deposits.

3. Delineation of buried and half-buried magmatic rocks

Based on the analysis of aeromagnetic anomalies and known magmatic rocks, we identified 3401 buried magmatic rocks of variable composition and extent. For example, we identified nine ultramafic–mafic rock belts, ten mafic rocks belts or regions, 27 intermediate felsic rock belts, and eight volcanic blocks in continental China.

The mafic and ultramafic rock bodies are mainly distributed along the deep Yarlung Zangbo River Fault belt, the Bangong Co–Nyima fault belt, the deep Erlian –Xi Ujimqin Banner fault belt, the deep Northern Qianlian Fault in Tibet, and the Erlian of Inner Mongolia and North Qianlian, whereas the rest are distributed in west Kunlun, Tianshan, west Junggar, east Tibet, Gansu Maqing, and Ailao Mountains.

The mafic rock bodies are widely distributed in north Tibet, southwest Sanjiang, Xikang–Yunnan, Baise and Rongjiang in Guangxi, Yinjiang, Daba Mountains, south Dabie Mountains in Guizhou, Bengbu in Anhui, and Qiemo in Xinjiang.

The intermediate felsic rock bodies are widely distributed in orogenic belts but not in continental blocks. In eastern China, volcanic rocks are mainly found in the periphery of the Songliao Basin, the Erlian Basin, the south Yellow Sea–Subei Basin, the Bohai Bay Basin, the eastern Zhejiang Province, and around the Hainan island, whereas, in western China, they are mainly found southern Sichuan, the northern Yunnan, middle Tibet, the Tarim Basin, Junggar Basin, and the Turpan–Hami Basin.

The map compilation not only reflects the known distribution of magmatic rocks but also shows the buried magmatic rocks. The study fills in the blanks in the distribution of magmatic rocks in continental China, which will facilitate the exploration of mineral resources associated with magmatism.

Regional geotectonic of continental China and aeromagnetic data

Methodology

The regional geotectonic map of continental China was compiled by considering the current understanding of plate tectonics. The map is based on the distribution of the metamorphic basement, the faults and sedimentary cover on the newly compiled 1:1000000 aeromagnetic maps as well as gravity, geological, seismic, remotes sensing, and other geophysical data. The structural units

on the map are divided into four groups. The first and second group are mainly based on aeromagnetic, gravity, and remote-sensing data and make up the tectonic map of continental China and adjacent regions (Ren, 2003; Pan et al., 2009). The third and fourth group are mainly based on the depth map of the magnetic basement as well as geological data.

Results and analysis

The regional geotectonic map of continental China shows the depressions and uplifts, and the depth and current distribution of the sedimentary cover.

The regional geotectonic map shows the geological structures covered by Quaternary rocks, the hidden structural units, and the depth of the basement and allows for new interpretations of the boundaries of tectonic units. In general, it is a very useful tool.

1. Division of regional structures

The map compilation (Figure 5) shows that there are eight structural units that are divided into orogenic and continental blocks (first-order division), 32 arc basins and continental and land blocks (second-order division), 85 basins, depressions, and uplift zones (third-order division), and 332 uplifts and depressions (fourth-order division).

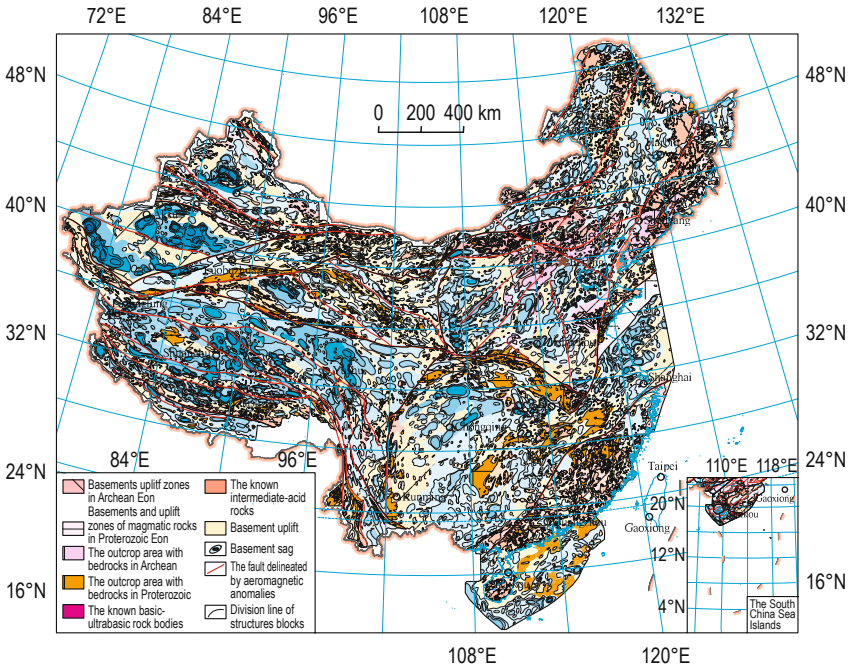

Fig.5 Regional geotectonic map of continental China based on aeromagnetic data.

2. New perspective

We offer new interpretations of the northern and western boundaries of the North China paraplatform, the northwestern and southeastern boundaries of the Yangtze paraplatform, and the eastern boundary of the Tarim continental block and the distribution of the Qiangtang, Cangdu, and Songpan–Ganzi orogenic belts.

(1) Northern and western boundaries of the North China paraplatform

Ren (2003) proposed that the northern boundary of the North China continental block is defined by the Helong–Huadian–south Siping–Chifeng–Bayan Oba–Lang mountain–Bayanruorigong–Jinta Line. However, on the magnetic maps, the middle segment of the northern boundary, defined by a previous study as the Siping–Bayan Oba Line, should be the Bayanruorigong –north Xianghuang Banner–Hexigten Banner–Xar Moron River Line, 80 km north of the previously defined boundary. The newly defined boundary follows a strongly magnetic belt. In the south side, the magnetic anomaly is consistent with the anomalies in the North China paraplatform, whereas the anomaly on the north side is comparable with the anomalies of the Tianshan –Xingan orogenic belt. The magnetic features suggest that the structures along the boundary belong to different tectonic units, have different basement properties, different sedimentary cover thickness, and reflect different episodes of tectonic and magmatic activity.

Moreover, the Cenozoic strata are well developed and are covered by Quaternary rocks along the boundary, which is reflected in the aeromagnetic data. Therefore, it is believed that a highly segmented deep fault belt exists along the boundary, which we named the deep fault belt of Bayan Oba–Xilamlun and constitutes the western segment of the northern boundary of the North China paraplatform. Hence, the northern boundary of the North China paraplatform should be the Helong–Huadian–south Siping–Xar Moron River–Hexigten Banner–north Xianghuang Banner Line.

The location of the western boundary of the North China paraplatform is controversial. Most believe that the Hexi Corridor and Alashan area belong to the North China paraplatform (Ren, 2003). However, from the aeromagnetic maps, the Hexi Corridor and Alashan area are characterized by NW-trending anomalies that are consistent with the anomalies in the Qilian Mountain area but different from the anomalies in the North China paraplatform. It is suggested that the boundary of the Hexi Corridor–Alashan area and the North China paraplatform should be the eastern Wulatehou Banner –Alxa Left Banner–Tongxin–Baoji Line. According to the features of the magnetic anomalies on both sides of the boundary, the anomalies of the Hexi Corridor and Alashan have characteristics of orogenic belts and the anomalies of the North China paraplatform have characteristics of continental blocks. The sedimentary rocks and fossils also suggest that the Alasha block does not belong to the North China paraplatform.

(2) The northwestern and southeastern boundaries of the Yangtze paraplatform

The Longmenshan fault is an important deep fault that divides the northwestern boundary of the Songpan –Ganzi block and Yangtze paraplatform. Based on the aeromagnetic map of the upward continuation, the aeromagnetic anomalies associated with the Longmenshan fault belt are blurred on the upward continuation map of 5 km and disappear on the upward continuation map of 10 km, indicating that the scale of the Longmenshan fault is not large and it is also shallow. However, from the analysis of the gravity and magnetic data, we suggest that the Longmenshan fault is a NE-trending frontal thrust belt rather than a deep fault belt. The gravity and magnetic anomalies between the Longmenshan and Songpan-Ganzi blocks are completely different but are very similar with those of the Yangtze paraplatform; thus, it is assigned to Yangtze paraplatform. In addition, the basement of metavolcanic rocks that span the Precambrian, Cambrian, and Middle Ordovician support the argument above. Therefore, it is suggested that the northwestern boundary of the Yangtze paraplatform should be the Wudu-Wenxian–Lixian–Kangding Line bounded by the Wudu–Kangding Fault.

The boundary of the Yangtze paraplatform and the South China block is complex and not easily recognizable. The conventional view is that the eastern boundary of the Yangtze paraplatform and the South China orogenic belt is the Jiangshan–Shaoxing fault, and the western boundary should be south of the Jiangnan uplift (Ren, 2003). However, it is clear that the magnetic anomalies associated with the boundary are very strong along the Beiliu–Linchuan–Jiangshan–Shaoxing Line. The strong anomalies are reflected by the Beihai–Jiangshan–Shaoxing fault belt and mark the contact of the Yangtze paraplatform and the South China orogenic belt. The gravity and magnetic anomalies on both sides of the fault belt are totally different. The weak magnetic anomalies on the northwestern side of fault belt resemble those of the Yangtze paraplatform, whereas the strong magnetic anomalies in the southeastern side of the fault belt are typical of orogenic belts. The boundary also divides structures and magmatic rocks. The strong Mesozoic magmatic activity formed intermediate felsic intrusive rocks, whereas the magmatic activity was weaker at the northwestern side of the boundary. Therefore, the southeastern boundary of the Yangtze paraplatform should be the Beiliu–Linchuan–Jiangshan–Shaoxing Line and the Beihai–Jiangshan–Shaoxing Fault.

(3) Eastern boundary of the Tarim paraplatform

The Tarim paraplatform is in the Taklimakan desert and its eastern boundary is considered the Arkin piedmont or the Qarqan River Line. However, the magnetic anomalies suggest that the eastern boundary of the Tarim paraplatform should be the Qira–Andrea–Tuogamu Line, bounded by the Qira–Weiya fault belt. The magnetic features on both sides of the boundary are quite different, suggesting different geological structures and basement properties, different styles of tectonic activity, and different sedimentary cover thickness; furthermore, they suggest that the block neither extends toward the east nor is in contact with the North China paraplatform. Because of the contrast in the amplitude variations of the magnetic anomalies in the Tarim paraplatform and the magnetic anomalies map for the Arkin, and the North and Tianshan Mountains, the eastern boundary of the Tarim paraplatform was clearly delineated.

(4) Distribution of the Qiangtang, Cangdu, and Songpan–Ganzi orogenic belts

Qiangtang and Cangdu in north Tibet are known as the Qiangtang–Cangdu block. However, the magnetic

anomalies clearly show that the Xuelian lake–Leiwuqi–Zuogong Line divides the magnetic field. The magnetic anomalies on both sides of the line are completely different. The trend of the western magnetic anomalies is mainly EW, whereas the eastern anomalies strike NW. The different trends are associated with the western Qiangtang block and the eastern Cangdu block. It is also suggested that the Qiangtang block and the Cangdu block belong to different structural zones based on the Jurassic stratigraphy and structures. In addition, the occurrence and development of the two blocks also differ, which is also reflected in the magnetic anomalies. The Jurassic-age EW-striking Qiangtang block has thickness between 2000 m and 7000 m, whereas the Permian-age NW-striking Cangdu block is only a few hundred meters thick (Xiong et al., 2013a).

The proposed distribution of the Songpan–Ganzi block is smaller than that proposed by Ren (2003). The Litang and Batang areas are extracted from the Songpan –south Ganzi–Litang block and are named the Litang arc basin with the Yushu–south Ganzi–Litang Line as the southern boundary. The proposed division is reflected by the magnetic anomalies in the Songpan–Ganzi block and Litang–Batang area. The former are associated with weak structural changes and magmatic activity, and thick sedimentary strata, whereas the latter are associated with intense structural changes and strong magmatic activity.

Conclusions

We reviewed the national 1:1000000 aeromagnetic maps and proposed several new interpretations of the magnetic features in relation with the regional geology. However, there are limitations because of the complexity of geological structures in continental China, the quality and quantity of the aeromagnetic data. The new map compilations do not cover most marine regions and neighboring countries. To obtain a continuous 1:1000000 magnetic map of China and its adjacent seas, it is important to have access to data from neighboring countries. Structural evolution, mineral and oil and gas resources have not been addressed in this study and remain to be studied in the future.

Acknowledgements

The work represents the efforts by many for many years at the China Aero Geophysical Survey and Remote Sensing Center for Land and Resources. We are wish to thank Fan Zhengguo, Zhang Hong-Rui, Huang Xu-Zhao, Zhou Daoqing, Xi Yufeng, Cai Yumei, Jia Weijie, Wang Wanyin, Wang Youwei, and many others. We also wish to thank Zhang Ming-Hua and Qiao Ji-Hua for their help in compiling the gravity anomalies map of continental China and the reviewers Meng Xiaohong, Lv Qingtian, Liu Yunxiang, Zhang Minghua for their comments.

References

Cheng, Y. Q, Fan, C. J., and Yang, M. G., 1994, Regional geology in China. Beijing: Geological Publishing House, 461−465.

Fan, Z. G., Huang, X. Z, Xiong, S. Q., et al., 2010, Technical requirement of magnetic materials application: Geological Publishing House, Beijing, 12−28.

Ge, X. H., Ma, W. P., Liu, J. L., et al., 2013, Prospect of researches on regional tectonics of China: Geology in China, **40**(1), 61−73.

Guan, Z. N., and An, Y. L., 1991, Quantitative interpretation of regional anomalies: Geological Publishing House, Beijing.

Guo, Z. H., Yu, C. C., and Zhou, J. X., 2003, The tangent technique of ΔT profile magnetic anomaly in the low magnetic latitude area: Geophysical and Geochemical Exploration, **27**(5), 391−394.

Huang, J. Q., Ren, J. S., Jiang, C. F., et al., 1985,Tectonic units and evolution in China: Science Press, Beijing, 80−98.

Huang, X. Z., and Guo, Z. H., 2007, Tangents method research of interactive aeromagnetic anomalies system: Geophysical and Geochemical Exploration, **31**(6), 572−576.

Li, T. D., 2006, Lithospheric tectonic units of China: Geology in China, **33**(4), 700−708.

Li, T. D., 2008, Geology map of central Asia and its adjacent regions: Geological Publishing House, Beijing.

Liu, G. D., 2007, Geodynamical evolution and tectonic framework of China: Earth Science Frontiers, **14**(3), 39−45.

Liu, S. P., Zhu, F. Y., Jiang, C. Y., et al., 1989, 1:4000000 aeromagnetic anomaly map of China land and adjacent sea regions: Geological Publishing House, Beijing.

Pan, G. T., Xiao, Q. H., Lu, S. N., et al., 2009, subdivision of tectonic units in China: Geology in China, **36**(1), 1−28.

Ren, J. S., 2003, New version geotectonic map in China-1:5000000 geotectonic map of China and adjacent region and specification: Acta Geosicientia Sinica, **24**(1), 1−2.

Ren, J. S., Wang, Z. X., Cheng, B. H., et al., 1999,The briefly specification of China and its adjacent area Tectonic map: Geological Publishing House, Beijing.

Sun, W. K., Huang, C. K., Ding, P. F., et al., 2001, Regional tectonic and metallogenic tectonic corpus of key metallogenic zone: Geological Publishing House, Beijing.

Teng, J. W., Pi, J. L., Yang, H., et al., 2012, The ponder for study the intension and locus of continental dynamics in China: Chinese Journal of Geophysics, **55**(3), 851−862.

Wan, T. F., 2011, Tectonics of China: Geological Publishing House, Beijing.

Wang, N. D., 2007, Some problems concerning 1:250 000 aeromagnetic series maps: Geophysical and Geochemical Exploration, **31**(5), 459−464.

Wang, N. D., Zhang, E. J., Yang, L. Y., et al., 2004, Aeromagnetic map of China and adjacent sea region (1:5000000): Geological Publishing House, Beijing.

Xiong, S. Q., Ding, Y. Y., and Li, Z. K., 2012, Characteristics of gravity and magnetic field in Xizang (Tibet) and new understanding on tectonic framework in Eastern Xizang: Geological Review, **58**(2), 201−207.

Xiong, S. Q., Ding, Y. Y., and Li, Z. K., 2013a, Gravity and magnetic field characteristics and their geological significance in Qiangtang basin, China: Oil Geophysical Prospecting, **48**(6), 999−1008.

Xiong, S. Q., Ding, Y. Y., and Li, Z. K., 2014a, Characteristics of China Continental magnetic basement depth: Chinese J. Geophys., **57**(12), 3981−3993.

Xiong, S. Q., Ding, Y. Y., and Li, Z. K., 2014b, A new understanding on the pattern of deep faults in Tibet and the southwestern Sanjiang area: Chinese J. Geophysics., **57**(12), 4097−4109.

Xiong, S. Q., Fan, Z. G., Zhang, H. R., et al., 2013b, Aeromagnetic series Map of China's Land and its specification (1:5,000,000): Geological Publishing House, Beijing.

Yang, H., and Liang, Y. M., 2011, Fault block and geological structure characteristics of China-1:5000000 aeromagnetic map of China land and adjacent sea area and specification: China Aero Geophysical Survey and Remote Sensing Center for land and resources, Beijing.

Zhao, W. J., 2009, Continental drift, plate tectonic and geomechanics: Acta Geosicientia Sinica, **30**(6), 717−731.

Zhu Y., 2002, Oblique magnetization tangent method and graphic feature point method: Geological Publishing House, Beijing.

Zhu, Y., 2013, Geotectonic and deep structures in China-Prelimenary interpretation of national 1:1000000 aeromagnetic maps: Geological Publishing House, Beijing.

Xiong Sheng-Qing is a senior geophysicist and professor. His research interests are in aerogeophysics and remote sensing. Presently, he is the chief geoscientist at the China Aero Geophysical Survey & Remote Sensing Center for Land & Resources.